Enlil is a name, not an abbreviation, like MAS & WSA

Comparison of Observations at ACE and *Ulysses* with ENLIL Model Results: Stream Interaction Regions during Carrington Rotations 2016 – 2018

L.K. Jian[1], C.T. Russell[1], J.G. Luhmann[2], P.J. MacNeice[3], D. Odstrcil[3], C.N. Arge[4], P. Riley[5], J.A. Linker[5], R.M. Skoug[6], J.T. Steinberg[6]

[1]Institute of Geophysics and Planetary Physics, University of California, Los Angeles, CA, 90095, USA.
[2]Space Sciences Laboratory, University of California, Berkeley, CA, 94720, USA.
[3]NASA, Goddard Space Flight Center, Code 674, Greenbelt, MD, 20771, USA.
[4]Space Vehicles Directorate, Air Force Research Laboratory, Kirtland Air Force Base, NM, 87117, USA.
[5]Predictive Science, Inc., San Diego, CA, 92121, USA.
[6]Space Science and Applications, Los Alamos National Laboratory, NM, 87545, USA.

Abstract

During the latitudinal alignment in May – July 2004, ACE and *Ulysses* encountered two fast-slow stream interaction regions (SIRs) over Carrington rotations 2016 – 2018, at 1 and 5.4 AU, respectively. More SIR-driven shocks were observed at 5.4 AU than at 1 AU, and three small SIRs at 1 AU merged to form a single and stronger interaction region at 5.4 AU. We compare the ENLIL model (version 2.6) results from CCMC with the ACE and *Ulysses* observations in detail, and demonstrate the predictive capability of the latest available models. The field polarity changes at all sector boundaries are captured by the models. The ENLIL model results are very susceptible to the differences in the input solar magnetograms (from MWO vs. NSO) and coronal models (WSA vs. MAS). Although the examined period is typical of the solar-cycle declining phase and no interplanetary CME was encountered, the timing of some simulated SIRs can differ from the observations by a couple of days at 1 AU and by up to six days at 5.4 AU. According to the 12 cases (two SIRs, two heliocentric distances and three rotations), the temperature and total pressure are often underestimated, while the density compression is often overestimated. Sometimes the models cannot well capture small-scale structures, such as shocks and small SIRs at 1 AU. The presence of non-potential active regions, the resolution limitation of solar magnetograms and models, and other factors can cause the discrepancy between models and observations. The coupled solar magnetogram – coronal model – heliospheric model chain needs further development to become an accurate research and/or forecasting tool. Higher-resolution solar and coronal observations, a mission closer to the Sun that tells us more about solar wind acceleration and the inner heliosphere, together with simulations with both greater spatial resolution and added physics, are ways to make further progress.

1. Introduction

Stream interaction regions (SIRs) are formed when fast solar wind overtakes and compresses preceding slow solar wind. In contrast to the interplanetary CMEs (ICMEs), SIRs persist throughout a solar cycle and are the predominant solar wind structure in the declining phase and around solar minimum (*e.g.*, Jian, Russell, and Luhmann, 2010). When solar conditions do not change substantially over a few solar rotations, SIRs can last for several solar shown in Figure 5. In comp... -ENLIL model, the NSO-MAS-ENLIL model has more pronounced differences between fast and slow wind in terms of various parameters except the plasma thermal pressure. The slow wind region is wider from the NSO-MAS-ENLIL model than from the NSO-WSA-ENLIL model. These differences could be in part because the speed derived from an *ad hoc* description is imposed at 30 Rs for the MAS-ENLIL model without taking into account the coronal field divergence as is done in the WSA model (Riley, Linker, and Mikic, 2001). Consistent with the differences at 0.144 AU, the 1-AU SIRs from the NSO-MAS-ENLIL model have a larger speed increase and are also wider than from the NSO-WSA-ENLIL model as shown in Figure 6(a). For both SIRs at 1 AU, the NSO-MAS-ENLIL run estimates the right magnitudes of fast wind speed, field and P_t enhancements, but underestimates the slow wind speed and overestimates compression of N_p and P_{dyn}. Associated with two fast wind regions at low latitudes over longitude 180°-300° at 0.144 AU (Figure 5) from the NSO-WAS-ENLIL and NSO-MAS-ENLIL models, there is a secondary speed increase and SIR on 18-20 June at 1 AU from the two models as illustrated in Figure 6(a), although the one from the NSO-MAS-ENLIL model is weak. ACE did not observe the secondary speed increase and associated SIR, so the models do not describe the rarefaction part after the SIR #4 correctly.

At 5.4 AU, all three runs predict a later arrival time for the two SIRs as shown in Figure 6(b), likely due to the overall underestimation of solar wind speed. Among the two SIRs simulated by three models, the lag of SIR #3 from the MWO-WSA-ENLIL model is the longest, about 5.5 days. For both SIRs, the order of SIR timing and the order of SIR strength among the three

* Speed profile is imposed at 1 Rs and mapped out along field lines to 30 Rs. So in some sense the divergence of the field is factored in.

1.2. Models

The Community Coordinated Modeling Center (CCMC) is a multi-agency partnership situated at the Goddard Space Flight Center of NASA. Through the effort of model developers and CCMC staff over years, several solar and heliospheric models have been installed and used for runs-on-request at the CCMC. In order to compare with the solar wind observations at both 1 and 5.4 AU, we use the ENLIL model, currently the only heliospheric model running beyond 5 AU at CCMC. Because the heliospheric model is designed for supersonic, super-Alfvénic, and low-β plasma, it needs inner boundary conditions from the coronal portion of either the Wang-Sheeley-Arge (WSA) model or the Magnetohydrodynamics-Around-a-Sphere (MAS) model.

The ENLIL model is a time-dependent 3D MHD heliospheric model developed by Dusan Odstrcil *et al.* Using a flux-corrected-transport algorithm, this model solves equations for plasma mass, momentum, energy density, and magnetic field (Odstrcil *et al.*, 2002; Odstrcil, 2003). The inner boundary is located at either 21.5 solar radii (Rs) for WSA coronal model as input or 30 Rs for MAS coronal model as input, both beyond the critical point of the solar wind. At the inner boundary, the solar rotation is added by imparting a corotational magnetic field component. The outer boundary can be adjusted to include planets or spacecraft of interest, with options of 2 and 10 AU available at the CCMC. In order to obtain results at 5.4 AU, we had to run the model all the way to 10 AU. We hope CCMC can add one more option of 5.5 or 6 AU, which can be useful to provide the solar wind condition for the investigation of Jupiter.

appropriate for Science paper?

The ENLIL model does not currently include corrections for any additional solar wind physics en route to 10 AU such as shock-related heating or interstellar pickup ion effects, which may become important between 5 and 10 AU. From the following comparison, we can see temperature is often underestimated even at 1 AU. So additional solar wind heating needs to be added. Whether it is needed for the heliospheric model or the coronal model or both requires further investigation. We choose the highest-resolution grid available, which is a uniform mesh of 1280×45×180 (radial × latitude × longitude, the other option is 1280×30×180) grid points for the 10-AU and 360°-longtitude heliosphere covering ±44° in helio-latitude, to concentrate grid points in the low-latitude region near the ecliptic plane. In other words, the spatial resolution of the ENLIL model for our runs is approximately 0.0078 AU (about 1.66 Rs) in radial distance, 2° in helio-latitude and helio-longitude. There are output options available at CCMC to obtain results calculated at Earth, *Ulysses*, and other planets or spacecraft. This is a new function added in 2010, and the trajectories of these objects are automatically taken into account.

X No. It is needed in Helio model.

The WSA coronal model combines a magnetostatic potential-field source surface (PFSS) model (Altschuler and Newkirk, 1969; Schatten, Wilcox, and Ness, 1969) and the Schatten current sheet model (Schatten, 1971). From the photosphere to the hypothetical sphere (the "source surface") where the solar wind takes over at 2.5 Rs, the PFSS approximation is used and the magnetic field lines are constrained to be radial. From 2.5 to 21.5 Rs, the Schatten current sheet model is incorporated in order to obtain a more realistic magnetic field configuration of the outer corona with the field lines diverging toward the current sheet (Arge *et al.*, 2004). This model uses an improved Wang and Sheeley empirical relationship (Wang and Sheeley, 1990a, 1990b; Arge and Pizzo, 2000; Arge *et al.*, 2002) to derive the solar wind speed at 21.5 Rs based on the relative expansion of the magnetic field lines from 1 to 21.5 Rs. Assuming ~~the~~ momentum-flux conservation and thermal-pressure balance, the WSA model also derives the density and temperature for the coronal region. Although the WSA model is an empirical model, it turns out to be very efficient and relatively accurate. Due to the current insufficient understanding of coronal physics, the WSA model is still widely used in the community.

The MAS coronal model is a time-dependent 3D MHD model covering 1-30 Rs developed by ~~the modeling group at the~~ Predictive Science Inc. (Riley, Linker, and Mikic, 2001; Riley *et al.*, 2001). Based on solar synoptic maps, ~~the~~ MAS model first uses a potential-field model and a Parker solar wind solution (Parker, 1958) to determine the initial plasma and magnetic field parameters, and then solves the Maxwell equations as well as the continuity, momentum, and energy equations to obtain a steady-state MHD solution. Because the MAS model at CCMC uses a simple polytropic energy equation, the highest numerically-derived speed in the solution is too slow (Lee *et al.*, 2009). Some *ad hoc* corrections for the expected velocity dependence on the distance from open field line boundaries are added to describe the speed at 30 Rs (Riley, Linker, and Mikic, 2001; Riley *et al.*, 2001). These corrections are consistent with the well-accepted views on the different origins of slow and fast wind. Similar to the WSA model, the density and temperature are obtained based on the conservation of momentum flux and the balance of thermal pressure.

As space weather fore

However, the long-term statistical comparisons may bury the details of how well models work for individual events. For example, the timing is earlier for some events and later for others, resulting in no systematic offset in statistical sense (Owens *et al.*, 2005), but users have no warning of how far off the timing can be. So in this study, we focus on SIRs during three CRs with no ICME encounters and quantify various aspects of the predictive capabilities of the models. In addition, after nearly 4-years use of the version 2.3a, the new version 2.6 of ENLIL model became available at CCMC in early 2010. It is thus timely to evaluate this new version of the ENLIL model. Such assessments can help improve the models' ability to describe solar wind conditions during times of quiet solar activity and provide the background conditions for transient events such as CMEs.

The inputs to both the WSA and MAS coronal models at CCMC are the full-CR synoptic maps derived from photospheric magnetograms, which are ground-based or near-Earth spacecraft line-of-sight (LOS) observations. These maps are different from daily updated synoptic maps which do not have specific start and end dates. Although the daily updated map incorporates the most recent observations, it is much more sensitive to the quality of individual magnetograms and susceptible to projection effects (Arge and Pizzo, 2000). In addition, because the ENLIL model generates a stationary solar wind solution for a given synoptic map, the 1-AU results have a ~4-day phase lag due to the solar wind propagation time. This can cause some poor correspondence between the model results and the spacecraft observations for the first few days of each CR.

At CCMC, there are three different sources of solar magnetogram for the WSA model:

At 5.4 AU, *Ulysses* [illegible] during 17-24 July with a very strong leading forward shock, presumably formed by the interaction and merging of SIRs #6-8 at 1 AU. This SIR has a maximum B of 3 nT and a maximum P_t of about 6 pPa, higher than the typical values for SIRs at this distance, 2.2 nT and 3.5 pPa (Jian *et al.*, 2008b), respectively. Figure 9(b) displays the comparison of *Ulysses* observations with the modeling results at 5.4 AU. All of the models predict later occurrence of the two SIRs, consistent with their overall underestimation of the solar wind speed. The NSO-MAS-ENLIL model gives the best timing match, despite of 2-day delay. The time separation between the two SIRs as well as the separation between the two sector boundaries from the three models are shorter than observed. In addition, none of the three models captures the negative polarity in the rarefaction region during 23-28 July.

All three models capture the forward-reverse shock pair of SIR #5 at 5.4 AU. At the leading edge of SIR #6, the simulated parameters from the MWO-WSA-ENLIL and NSO-WSA-ENLIL models change too gradually to mimic the observed forward shock. The trailing edge of SIR #6 cannot be classified as a reverse shock because the observed temperature and field features do not have the shock signatures, but the NSO-MAS-ENLIL model produces a reverse shock. This suggests the physical processes in the real solar wind are more complicated than what can be described in the models and some of the SIR-driven shocks are not well-developed at 5.4 AU and can be missed by a single-point observation.

For SIR #5 at 5.4 AU, the three models underestimate the background solar wind temperature by more than one order of magnitude, and slightly underestimate B and P_t. Combining the underestimation of solar wind speed and overestimation of density, the P_{dyn} estimation is about right. The temporal profiles of N_p, B, P_t, and P_{dyn} are not symmetric and have a sharper increase at the leading part. The MWO-WSA-ENLIL and NSO-MAS-ENLIL models capture such features. For SIR #6, the NSO-MAS-ENLIL run produces the strongest event

* Enlil doesn't use B from either the MAS or WSA solutions it is set to some large [illegible] value and the location of the HCS is traced out. (at least the version you probably ran at the CCMC)

models both change from 1 to 5.4 AU. Using the maximum P_t to approximate the strength, the SIR #3 from the MWO-WSA-ENLIL model is the weakest among the three models at 1 AU but the strongest at 5.4 AU; the model generating strongest SIR #4 changes from the NSO-WSA-ENLIL model at 1 AU to the NSO-MAS-ENLIL model at 5.4 AU. From 1 to 5.4 AU, as the stream interaction strengthens, the ratio of the simulated SIR duration to the observed duration usually decreases, as listed in Table 1, except the NSO-WSA-ENLIL model for CR 2017.

With the radial evolution of a SIR, the pressure waves bounding it steepen into forward and reverse shocks at 5.4 AU, as marked by magenta dashed lines in Figure 6(b). Considering the limited resolution of the solar synoptic maps and coronal/heliospheric models, the leading and trailing edges of the two SIRs from the three models almost mimic a pair of forward-reverse shocks except the SIR #4 from the MWO-WSA-ENLIL model, where the parameters change gradually at the edges probably related to a small speed difference between fast and slow streams and a weak resultant stream interaction. None of the three runs captures the observed double forward shocks leading SIRs #3 and #4 at 5.4 AU.

For the two SIRs at 5.4 AU, all the three models underestimate the solar wind speed and ambient temperature, while overestimating the density compression. The NSO-WSA-ENLIL and NSO-MAS-ENLIL models give about the right magnitudes of field and P_t increases for SIR #3, while the MWO-WSA-ENLIL model overestimates these enhancements. For SIR #4, the MWO-WSA-ENLIL and NSO-WSA-ENLIL models underestimate the peak field and P_t, but estimates a right amount of P_{dyn} enhancement, while the NSO-MAS-ENLIL model overestimates all of these peak values. These models cannot capture some of the observed time variations of N_p, B, P_t, and P_{dyn}. The solar wind of SIR #4 from the NSO-WSA-ENLIL run is accelerated in two steps, and there are two N_p increase regions, in contrast to the observations and other two models. This seems to be due to the radial evolution of the two SIRs over 14-20 June at 1 AU.

From the above comparison, the differences due to the different coronal models for CR 2017 can be as significant as the differences due to different solar synoptic maps. We use the stream interface time, duration, plasma, field, and combined parameters listed in Table 1 to evaluate the models quantitatively. The italic number marks the model that best matches the observations. Considering the simulation-to-observation parameter ratios, counting the stream interface time discrepancy with a weight of 2, and also considering the above comments about the detailed time profiles, we give an objective assessment of the model's ability to reproduce the SIR, with 1 to 3 in order of decreasing capability. For example, about SIR #3 at 1 AU, the NSO-WSA-ENLIL model has the best timing match (a weight of 2) and the best match for other four parameters, so its success count is 6, more than the other two models, and we rate the model as 1 for this event. In short, the best model rating 1 is usually the one with the most italic numbers and with the best timing match. For the two SIRs at 1 and 5.4 AU during CR2017, the MWO-WSA-ENLIL model consistently rates number 3, indicating a bad fit for this CR. The NSO-WSA-ENLIL model reproduces SIR #3 best at both distances, while the NSO-MAS-ENLIL model fits SIR #4 best at both distances. The better results obtained using the NSO synoptic map is probably because NSO has more sensitive instruments and better corrections to the polar field than MWO for this CR.

2.3. CR 2018

As we did for CR2017, we requested three CCMC runs for CR 2018: the MWO-WSA-ENLIL, NSO-WSA-ENLIL, and NSO-MAS-ENLIL runs. Figure 7 compares the photospheric synoptic maps from MWO and NSO in the first panel. Analogous to the comparison in Figure 4, the NSO map displays more small-scale structures than the MWO map, and the WSA coronal model results at 21.5 Rs based on them are remarkably different. The derived HCS from the NSO-WSA model is tilted to higher latitudes than the HCS from the MWO-WSA model, by about 15°, probably because the field from the low-latitude active regions and coronal holes in the NSO-WSA model is stronger. The high-latitude solar wind from the NSO-WSA model is faster than from the MWO-WSA model. The speed distributions in the slow wind regions over longitude 240°-360° are fairly different between the two models.

Figure 8 illustrates the color contours of the solar wind speed, number density, particle temperature, plasma thermal pressure, and magnetic field intensity from the three runs at 0.144 AU, the common innermost boundary of the heliospheric part. The NSO-WSA-ENLIL model looks like an intermediate solution between the other two models, in terms of the differences of V, T_p, and B between the slow and fast wind. The HCSs from the NSO-WSA-ENLIL and NSO-MAS-ENLIL models are both more tilted than the one from the MWO-WSA-ENLIL model, while the slow wind region from the NSO-MAS-ENLIL model is considerably wider than from the other two models. The structure at 0.144 AU from the NSO-WSA-ENLIL model is more complicated than from the other two models, including two fast streams over the longitude 160°-280°. The weak-field region over longitude 240°-360° from the MWO-WSA-ENLIL model is smaller than from the other two models.

Figure 9(a) compares the ACE observations (black dots) and simulation results (color curved and 0.40R [...]ates, the unit vector **R** points away from Sun center through the spacecraft; **T** is formed by the cross product of the solar rotation axis and **R** and lies in the solar equatorial plane; and **N** is the projection of the solar rotation axis on the plane of the sky. As the two shocks roughly propagate against each other, these SIRs are expected to expand and merge into one SIR, as confirmed by the *Ulysses* observation at 5.4 AU.

At 1 AU, the NSO-WSA-ENLIL model predicts the timing of SIRs #5 and #6 best, consistent with its best estimation of the overall solar wind speed among the three models, as shown in Figure 9(a). The NSO-MAS-ENLIL model (blue line) predicts a later interface time for both SIRs #5 and #6, probably because its simulated fast wind interval is too short and the slow wind lasts long although the maximum fast wind speed is overestimated by nearly 100 km s^{-1}. The MWO-WSA-ENLIL model (red line) generates a 1.5-day late timing for SIR #5, probably due to its overall underestimation of solar wind speed. The simulated magnetic field polarity and

* I'm not sure that the concept of 'tilt' is appropriate unless the solar field is a simple dipole, tilted wrt the rotation axis. Then the loci is a sinusoid on a lat/lon map. Otherwise 'maximum extent' might be a better description.

among the three models, and the parameters are closest to the observations too. Even so, the P_t is only one third of the observed. This model also mimics the observed non-symmetric temporal variations of N_p, B, P_t, and P_{dyn}, while the other two models produce a more gradual increase for these parameters. For both SIRs, the order of SIR timing and the order of SIR strength among the three models both change from 1 to 5.4 AU.

At both 1 and 5.4 AU, the difference between the two runs using different solar synoptic maps can be as prominent as the difference caused by different coronal models, similar to what concluded from the comparison of CR 2017. Based on the cumulative assessment of multiple parameters, for SIRs #5 and #6 at two heliocentric distances, the NSO-MAS-ENLIL model is rated number 1 for three items (Table 1), indicating it predicts the CR 2018 features best, while the MWO-WSA-ENLIL model is rated number3 for three items and thus does not do as good a job matching the observations for this CR.

3. Discussion and Conclusions

We have chosen three CRs 2016 – 2018 in 2004, when solar wind stream structures are observed by both ACE and *Ulysses* at 1 and 5.4 AU, respectively. No ICMEs occurred in this time window. The radial variations of the six SIRs agree with our statistical results for 1-AU and 5.4-AU SIRs in Jian *et al*. (2006, 2008b). From 1 to 5.4 AU, the slow streams are accelerated, while the fast streams are decelerated, and more shocks, usually forward-reverse shock pairs, are driven. In CR 2018, three small SIRs appeared during 10-22 July at 1 AU, while only one corresponding SIR was found at 5.4 AU, implying the interaction and merging of small SIRs along with their outward propagation. This at least partially explains why we see fewer SIRs at a greater heliocentric distance (Jian *et al*., 2008b).

Comparing the observations and model results, we conclude that the ENLIL model can generally reproduce the sector boundaries and field polarity, and roughly capture the occurrence and features of SIRs, but it cannot precisely predict the timing of the SIRs and sector boundaries. From Table 1, in terms of timing, the best performer is the NSO-WSA-ENLIL model (four times producing the best match

s and are called corotating interaction regions, or CIRs (Sm
re, being able to capture these SIRs is an important elemen
dation of successful space weather forecasting. Having co
multiple heliocentric distances (Jian *et al.*, 2006, 2008a, 20
ng here several SIRs at 1 and 5.4 AU in depth to evaluate t
duce these SIRs and their radial variations.

servations

the first spacecraft to study the Sun and solar wind at nearly
in a trajectory highly inclined to the ecliptic plane (Wenzel
ears, *Ulysses* accomplished nearly three complete orbits in i
n passes at 5.4 AU in February 1992, April 1998, and June 2
nd observations was poor for the first aphelion pass. But du
n passes, *Advanced Composition Explorer* (ACE) provided c
ing at 1 AU, enabling us to study the radial evolution of indi
ry latitudinal alignment during the two aphelion passes was a
ind structure was too complicated and varied dramatically fro
periods of strong solar activity; at other times no clearly ident

our surveys of SI ... 2006

here, we chose the option of 1280×45×180 grid, which is the highest available at the CCMC. The corresponding model resolution is only 0.0078 AU (about 40 minutes assuming solar wind speed of 500 km s^{-1}) in radial distance, 2° in longitude, and 2° in latitude for the 10-AU heliosphere. Converting the 360°-longitude range to one CR, the temporal resolution is about 3.6 hours. Models with such low resolution cannot capture small-scale structures in the solar wind, in particular, shocks and the boundaries between fast and slow streams which exhibit sharp changes of parameters within a few minutes. For example, none of the shocks reproduce the double forward shocks during CR 2017.

a simulation region spanning

To resolve the small-scale structures and obtain variations of such as 10-minute resolution in the simulation, the grid points in the radial and longitudinal directions need to be approximately 5120 and 4000 for a 10-AU heliosphere, or 1024 and 800 for a 2-AU heliosphere. At present, the finest grid for 2-AU ~~heliosphere at the CCMC~~ is 1024×120×360, so the desirable high resolution grid is possible for some test runs. This discussion also raises the issue of the outer boundary. As mentioned in the introduction, *Ulysses* provided an important and unique solar wind data set with its aphelion just beyond 5 AU, its high latitude perspective, and its long-term observations. We hope the CCMC can add the option of 5.5 or 6 AU for the outer boundary of the ENLIL model. This can greatly benefit the investigation of the space environment for Jupiter, for example.

Because all observatories have their own special ways of constructing and correcting the synoptic map~~s~~ ~~(~~e.g., Neugebauer *et al.*, 1998; Arge and Pizzo, 2000; and references therein), the ~~ENLIL~~ models using synoptic maps from different sources can generate results with significant

MAS and WSA

(as noted earlier, Enlil doesn't even use a real B!)

differ from the order at 1 AU. Because the same SIR at two heliocentric distances are not completely independent cases, we definitely need to study more CRs to obtain more convincing statistics and to find out which observatory and which coronal model can statistically reproduce SIRs best.

It would also be helpful to have access to inter-calibrated magnetograms from multiple sources, which have a higher level of confidence in the absolute field strength and also validated corrections to the observationally challenging polar fields (Owen *et al.*, 2005; Lee *et al.*, 2009). Before such boundary data becomes available, our comparison suggests that when we do not know which solar synoptic map or which coronal model is more reliable, it is instructive to run the heliospheric model using multiple solar magnetograms and multiple coronal models. The lack of a definitive best input is also why the CCMC has added GONG as an additional source of input. The CCMC also has plans to take the magnetograms from the Michelson Doppler Imager (Scherrer *et al.*, 1995) on board the Solar and Heliospheric Observatory (SOHO) spacecraft, and from the Solar Dynamics Observatory (SDO), which has much higher resolution solar observations than before.

Because we do not have *in situ* observations for the coronal model domain, it is difficult to evaluate the different coronal models quantitatively. At present, we can use the heliospheric model results evolved from the coronal-model outer boundary, or the images in extreme ultraviolet (EUV) and soft X-rays to indirectly assess the coronal models. The CCMC can in principle provide simulated coronal hole maps and/or polarized brightness maps as output from the coronal models used in WSA-ENLIL and MAS-ENLIL, as what has been provided for STEREO support by the Predictive Science. These maps can be compared with the coronal observations as a sanity check on the coronal models. Future missions, such as the Solar Orbiter (Marsch *et al.*, 2005) or Solar Probe Plus (McComas *et al.*, 2005), will make critical measurements in the outer corona and mid-range inner heliosphere that will also greatly benefit coronal and heliospheric models.

ENLIL runs at CCMC are conducted promptly following submission, usually taking
uple of days. This interface to the models provides a uniquely useful and convenient
nalyzing and predicting the solar wind and planetary space environment. In comparison
earlier model ENLIL 2.3a for the same time periods (not shown here), we find the new
.6 can generate stronger enhancements of solar wind density, field, and pressures, but
ver temperature. In comparison with observations, the new code can give better field and
estimations, but worse temperature matches. As the model codes are constantly updated
developers, it is important to run and validate the new versions in systematic ways to test
ts of the changes made. Since we ran the case studies described above, the CCMC has
d the number of coronal and heliospheric models that it serves, and now includes, e.g.
e Weather Modeling Framework from the University of Michigan. More model
tions and more sources of synoptic maps will soon be offered at the CCMC. We will

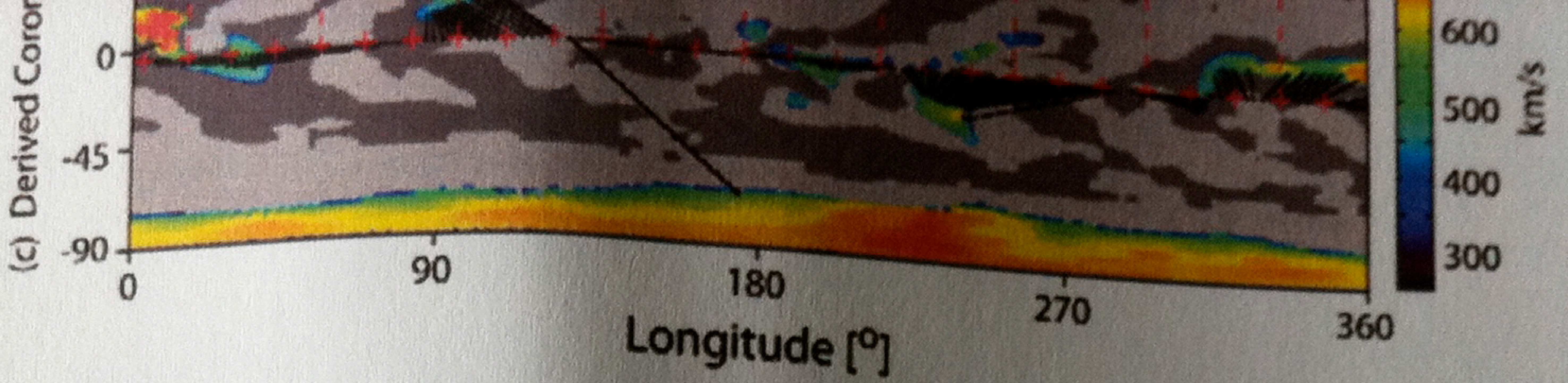

Figure 1 The MWO photospheric magnetograph and the WSA coronal model results for CR 2016. The panels from top to bottom: (a) the MWO photospheric magnetograph; (b) the derived solar wind speed at 21.5 Rs, *i.e.*, about 0.1 AU; (c) the derived coronal hole areas with the solid black lines connecting the outer coronal boundary at 21.5 Rs and its source regions at the photosphere. In panel (b), the two dashed black lines mark the latitudinal range covered in Figure 2. In panel (c), the colored dots represent photospheric footpoints of the open field lines. The areas shaded light (or dark) gray denote closed field lines with positive (or negative) radial magnetic field in the photosphere. The color scale indicates the solar wind speed at 21.5 Rs (related to the expansion factor, see Arge *et al*., 2004, and references therein) associated with the flux tubes. In all the three panels, the + symbol marks the daily position of the sub-Earth point on the Sun, and the time sequence is from ~~left to right~~.

right to left

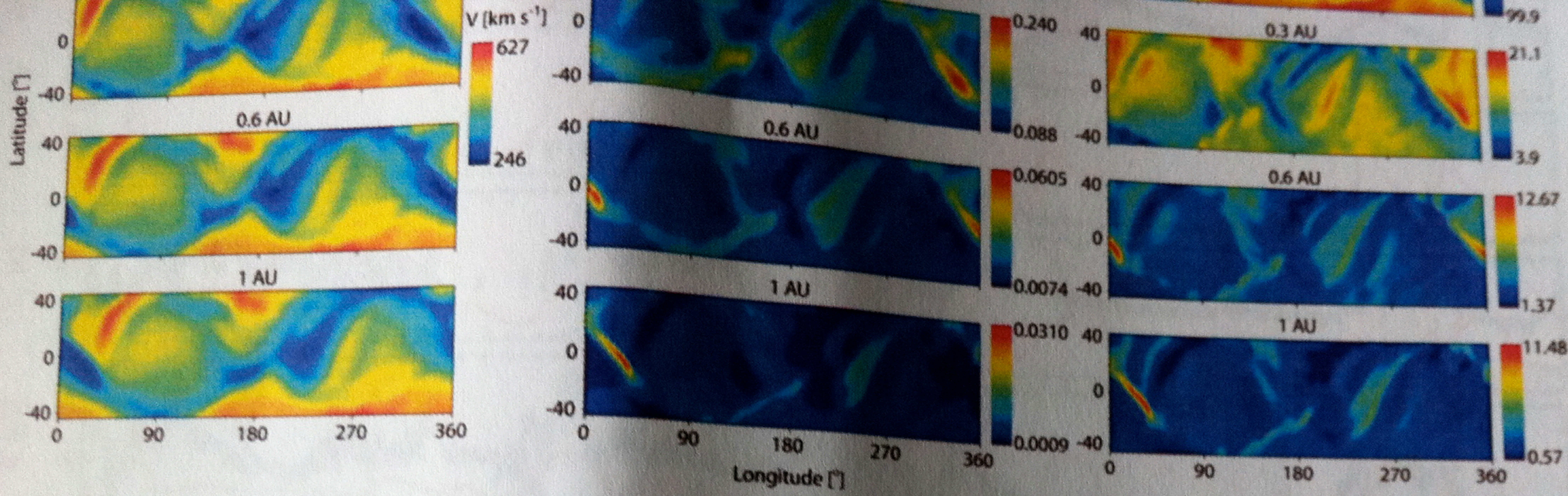

Figure 2 The color contours of (a) solar wind speed, (b) plasma thermal pressure, and (c) magnetic field intensity from the MWO-WSA-ENLIL model at 0.1, 0.3, 0.6, and 1 AU. The indication of different color is given by the color scale. The longitudinal variation from 0° to 360° represents the temporal variation throughout one CR.

?

Spatial variation ?

CR 2016

Figure 3 Comparison of ENLIL model results with (a) ACE observations during 2-29 May 2004 and (b) *Ulysses* observations during 12 May – 7 June 2004. From top to bottom: solar win speed *V*, proton number density N_p, proton temperature T_p, magnetic field intensity *B*, magnetic field polarity, total pressure P_t, and dynamic pressure P_{dyn}. The black dots are *in situ* spacecraft observations; the solid red lines give the model results. The spacecraft positions in the heliographic inertial (HGI) coordinates are provided at the bottom. Considering the orbital peri at 5.4 AU is much longer than the solar rotation period, we use the solar equatorial rotation period of 26 days as the time window. The magenta dashed vertical lines mark the observed shocks, labeled f.s. for forward shock and r.s. for reverse shock.

I understand what you mean but this is confusing/vague. It's probably not necessary.

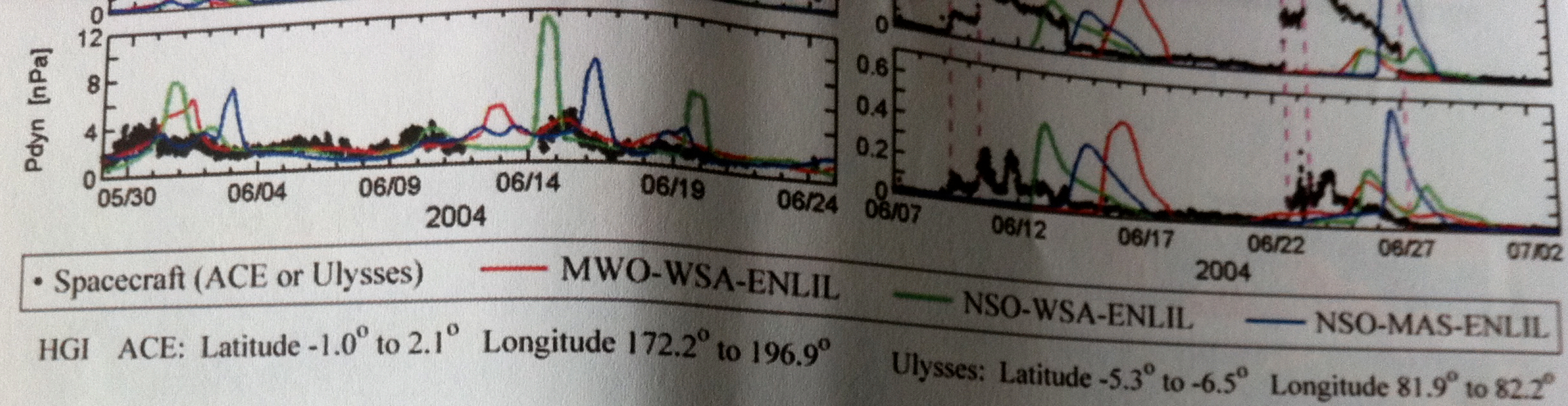

Figure 6 Comparison of the ENLIL simulation results with (a) ACE observations at 1 AU during 29 May – 25 June 2004 and (b) *Ulysses* observations at 5.4 AU during 7 June – 3 July 2004. The black dots denote spacecraft observations; the red, green and blue lines indicate the results from the MWO-WSA-ENLIL, NSO-WSA-ENLIL, and NSO-MAS-ENLIL models, respectively. The spacecraft location are given at the bottom. From top to bottom are the V, N_p, T_p, B, magnetic field polarity, P_t, and P_{dyn}. The magenta dashed vertical lines mark the observed shocks.